Heat recovery potential from ventilated passive and active facades: A numerical study

Mohammad Rahiminejad, Dolaana Khovalyg.

Ecole Polytechnique Fdérale de Lausanne (EPFL), Laboratory of Integrated Comfort Engineering (ICE), CH-1700 Fribourg, Switzerland, mohammad.rahiminejad@epfl.ch.

Abstract. A ventilated air-space behind external claddings can potentially affect the thermal performance of the entire building structure. In particular, in the Building Integrated Photovoltaic (BIPV) facades, ventilated cavities are typically present between the PV panels and the walls of the building. The airflow in the cavity can remove the generated heat behind the active external cladding, which could be eventually used as an additional source for heat recovery. In this study, the heat recovery from a ventilated air-space behind passive (wood) and active (BIPV) facades are investigated using transient simulations.

The numerical model used in this study is validated against experimental measurements carried out in a building prototype located in the Smart Living Lab in Fribourg (Switzerland). The original façade is made of wooden cladding that is separated from the wall core incorporating a ventilated cavity. To study the impact of façade type on the results, the external cladding is virtually replaced with typical polycrystalline PV panels. The analyses are performed for representative days in the winter and summer of 2021 using recorded weather data on the test building. The results are examined in terms of the temperature distribution of the layers in the wall assembly, heat flux through the indoor space, airspeed in the cavity, and heat flow in the air gap. The potentials for heat recovery per day of interest are also calculated and compared. It was shown that the heat recovery from the cavity behind the BIPV façade could become equal to 5341 kWh on a representative summer day, which is considerably higher compared to the value obtained for a passive cladding. The results highlight the potential for harvesting heat from the ventilated air gaps behind passive and active facades. The outcome of this study highlights the need for the integrated vision for energy-savings at the building scale.

1. Introduction

The introduction of wall designs that incorporates air-spaces behind claddings can reduce energy use in buildings by impacting the thermal performance of the entire wall structure [1-5]. The thermal resistance caused by the ventilated air-space depends on multiple parameters, and it can be measured to evaluate the contribution of the air-space to the total R-value of the assembly [6-8]. In North America, the air cavity is used to eliminate capillary flow between the cladding and sheathing and provide ventilation to remove moisture [9]. In the European community, the ventilated façade is usually used in refurbishment projects to reduce the heat loss through the building envelope and improve the thermal resistance of the wall [10]. Traditionally, ventilated façade systems have been predominantly used in colder climates of Europe and North America to reduce the load on the heating systems by warming the airflow in the cavity caused by the Sun.

More recently, the ventilation of the warm air due to the stack effect of natural air circulation inside the cavity has begun to be used in warmer climates such as Australia to benefit from the reduced solar heat gain of the building; and consequently, reducing the load on the cooling systems [11].

In addition to the aforementioned advantages, the ventilated air gaps behind external claddings can be considered as a possible source for heat recovery. The wasted heat from the air cavity can be harvested and utilized for the HVAC system in the building, which can eventually reduce the operational energy of the building [12].

The ventilated cavity can be incorporated in both passive (traditional) and active Building Integrated PV (BIPV) facades. Particularly in the latter type, the heat flow removed from the ventilated air-space can reduce the temperature of the PV modules and enhance the electrical efficiency of the BIPV system

[13]. Despite the prevalence of studies on the heat removal from the air gap behind the traditional claddings [14, 15] and BIPV facades [16-19], research works that compare the heat recovery from the ventilated air-spaces behind passive (traditional) and active (BIPV) claddings in a real-scale building are still lacking. Most of the previous works have only focused on the heat recovery potential behind external claddings in a small scale wall structure. In the present study, a numerical transient 2-D model is employed to investigate the heat recovery of the naturally ventilated air-space behind passive (wood) and active (BIPV) facades implemented in a full-scale building prototype. The original façade of the test building is made of wooden cladding, and it is virtually replaced with typical polycrystalline PV modules to study the impact of the façade type on the results. The analyses are performed for two representative days, one in the winter and one in the summer of 2021, using weather data monitored on the test building.

2. Methodology

2.1 Case Study: CELLS

The test building that is used for the simulations is a shared research facility CELLS (Controlled Environment for Living Lab Studies), in the Smart Living Lablocated in Fribourg, Switzerland (Figure 1). The test building is composed of two identical rooms with different thermal inertia walls. The low inertia room is east-oriented, and the high inertia room is west-oriented. The wooden cladding of the wall assembly is separated from the wall core with an air-space behind the façade. The cavity is naturally ventilated by the airflow that can freely move through the bottom and top openings. In this study, the heat flow removal from the ventilated cavity behind the west-oriented wall is investigated.

Fig. 1 – Façade of the building prototype CELLS (Fribourg, Switzerland).

2.2 Numerical model of the wall structure

To model the transient heat transfer mechanisms through the entire structure, a 2-D finite-difference method is employed. The system is divided into multiple control volumes, and a two-dimensional nodal network with 5 nodes along with the height and 3 nodes through the depth of each layer in the geometry is created. The model is elaborated in detail by Rahiminejad & Khovalyg [20] and has been validated for wall structures with both passive and active facades using experimental measurements. Figure 2 shows a schematic of the ventilated wall assembly. The wind effect and stack effect are mechanisms that naturally drive airflow in the cavity and cause a temperature difference between the top and bottom openings [21]. The heat flow through the air gap per area of the cavity (equation (1)) is a function of the density and specific heat capacity of the airflow, airspeed in the cavity and its temperature gradient from top to bottom:

$$q_{cav} = \rho V_{cav} c_p (T_t - T_b) \qquad (1)$$

The heat flow removed from the cavity can also affect the heat flux through the interior surface of the wall (equation (2)), which is a function of the heat transfer coefficient and the temperature difference between the interior surface and indoor space:
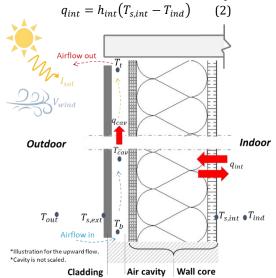
$$q_{int} = h_{int}(T_{s,int} - T_{ind}) \qquad (2)$$

Fig. 2 - Schematic representation of a ventilated wall.

In total, four simulations are performed considering representative days in winter and summer of 2021; 2 for wall structures with original passive cladding (wood) of the building prototype, and 2 for a similar wall assembly but with the external cladding entirely replaced with polycrystalline PV modules. As shown in Figure 3, the PV module consists of tempered glass, photovoltaic cells encapsulated between ethyl vinyl acetate (EVA) layers, and a polymer back sheet. The thermo-physical properties of the layers used in the simulation are summarized in Table 1.
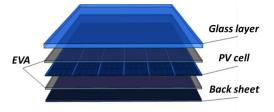

Fig. 3 – Layers used in the PV module.

The simulations are performed using the data of 8 hours in advance of the chosen day to ensure convergence of the simulations prior to the day of interest. Assumptions made in the calculation process are: (i) fully developed flow across the width of the air cavity, (ii) no airflow infiltration between

the photovoltaic modules along with the height of the wall, and (iii) negligible effects of thermal bridges.

Tab. 1 - Thermo-physical properties of the test wall*.

Material (exterior to interior)	d (m)	k (W/m·K)	ρ (kg/m³)	c_p (J/kg·K)
Passive facade				
Wood	0.024	0.10	450	1800
Active façade				
Tempered glass	0.0036	1.8	3000	500
EVA	0.0004	0.35	960	2090
PV cell	0.0004	148	2330	700
Back sheet	0.0004	0.13	1450	1650
Wall core				
Insulation	0.180	0.03	15	1404
Timber hardwood	0.140	0.13	471	1600
Earth brick	0.050	0.79	1900	1100
Jute coating	0.015	0.80	1600	1450
Air-space	0.070	varies	varies	varies

*Only selected properties are mentioned. See [20] for more details.

2.3 Weather Data

The weather data of two representative days in Fribourg, Switzerland, in winter (March 02nd) and summer (July 29th) of 2021 are used as the outdoor conditions. The diurnal variations of outdoor air temperature, vertical solar radiation [22], and wind speed are shown in Figure 3. The data are collected using a weather station installed on the facade of the test building (Figure 1). The weather station includes an air temperature sensor (S-THB-M002, Onset), Davis® wind speed and direction sensor (S-WCF-M003, Onset), and silicon pyranometer for global horizontal irradiance (S-LIB-M003, Onset).
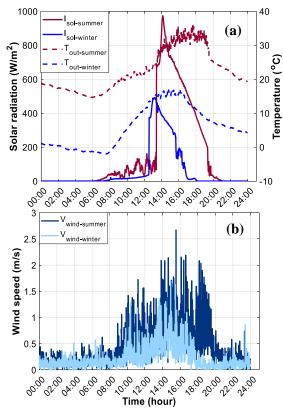

Fig. 3 – (a) Outdoor air temperature and vertical solar radiation, (b) Wind speed for representative days in winter (March 02nd) and summer (July 29th) of 2021.

The sensors in the weather station are connected to a micro station data logger (H21-USB, Onset) to record data at 1-minute intervals. Indoor air temperatures are assumed to be equal to 21°C in winter and 26°C in summer [23].

3. Results

In this section, the results of the simulations are presented in terms of temperature distribution through the wall structures, heat flux through the interior surface, airspeed in the cavity, and heat flow in the air-space. The results shown in the following subsections, unless it is indicated, are averaged for 5 nodes along with the height of the wall assembly.

3.1 Temperature distribution on the surfaces

The daily evolution of temperature on the exterior surface of cladding with both passive and active facades is presented in Figure 4(a). According to the results, the surface temperature of the passive façade reaches up to 38°C in winter and 62°C in summer. The corresponding values for the active façade are 54°C and 98°C, respectively, which are 16°C and 36°C higher compared to the passive cladding. The high rear surface temperature of the active façade in summer is due to the assumption of a closed-joint BIPV façade (i.e., the connections between the PV panels are with no air infiltration). Similar values are reported in other works [24-25], which would strongly affect the efficiency of the panels. The difference between the maximum surface temperature of passive cladding with the maximum outdoor temperature is equal to 20°C in winter and 27°C in summer. In the case of using an active façade, the values become 36°C in winter and 63°C in summer. These differences imply the impact of solar radiation on the surface temperature of the external cladding. Comparing the plots in Figure 4(a) with the weather data shown in Figure 3 reveal that the surface temperature of the external cladding with passive façade generally follows the diurnal outdoor temperature, while the variation in solar radiation during a day has a predominant impact on the surface temperature of the external cladding with active façade. This could be attributed to the difference in the thermal properties of the layers used in the passive and active façades. In particular, the high thermal transmittance and solar absorptivity of the glass layer in the BIPV façade exposed to outdoor could result in a more pronounced effect of solar radiation on the surface temperature of the active façade. Moreover, it can be seen from the plots in Figure 4(a) that the difference in the thermal mass of the external claddings, defined as volumetric heat capacity × volume of the material, has caused a time delay of up to 3 hours in winter and 4 hours in summer in the maximum surface temperature between the passive and active façades.

The temperature of the interior surface of the jute coating that is adjacent to the indoor space is shown in Figure 4(b). According to the results, the difference between the temperatures of the interior surfaces in wall structures with passive and active

façades reaches up to 0.1°C in winter and 0.4°C in summer. The higher value in the latter is due to the higher difference between the surface temperature of the two claddings in summer, which has been propagated through the entire wall structure. Moreover, the results indicate that the maximum deviation of the interior surface temperature from the fixed indoor temperatures in winter and summer is equal to 0.4°C. The plots in Figure 4(b) show that the interior surface temperature of the wall structure with both passive and active façades is almost always lower than the fixed indoor temperature in winter, which is due to the temperature gradient through the wall assembly caused by the lower outdoor temperature compared to the fixed indoor temperature. In summer, however, the temperature on the interior surface of the wall with passive cladding is lower than the indoor temperature, while it becomes higher (from 1:00 to 6:00, and from 17:00 to 24:00) in case of using an active façade. This is mainly due to the higher surface temperature of the external cladding in the latter. Furthermore, the impact of the thermal mass of the external cladding is noticeable in the diurnal behavior of the interior surface temperature. In other words, the amplitude of the interior surface temperature is higher in the wall structure with the active façade compared to the wall assembly with passive cladding, which is due to the lower thermal inertia of the former one.
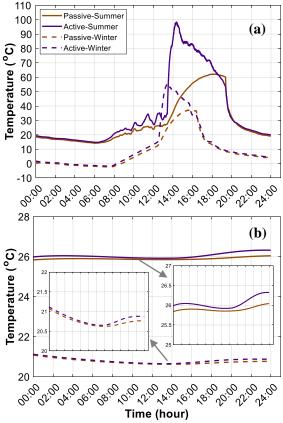

Fig. 4 – Temperature distribution averaged along with the height of the wall (a) Exterior surface of cladding, (b) Interior surface of jute coating.

The evolutions of the airflow temperature in the cavity at the middle height and top opening are shown in Figure 5. The airflow temperature at the bottom opening in each time step is assumed to be equal to the outdoor temperature and is not shown here. According to the results in Figure 5(a), the airflow temperature in the middle of the cavity behind the passive cladding reaches up to 20°C in winter and 40°C in summer. In case of using the BIPV façade, the values are 20°C and 30°C higher compared to the passive façade. The results in Figure 5(b) indicate that the airflow temperature at the top opening is higher compared to the middle of the air-space. The difference is 8°C for passive cladding in winter and summer conditions. By replacing the original cladding of the test building with PV panels, the difference between the airflow temperature at the top opening and in the middle of the cavity becomes 18°C in winter and 30°C in summer. The wind effect and stack effect are more pronounced in summer compared to winter. The airflow in the air-space becomes warm at the time when the wall structure is exposed to the Sun. Consequently, the temperature of the airflow becomes higher at top points compared to the lower points in the cavity. This phenomenon is more noticeable in the cavity behind the active façade, which is due to the lower thickness and higher thermal conductivity of the PV panel compare to the wood.
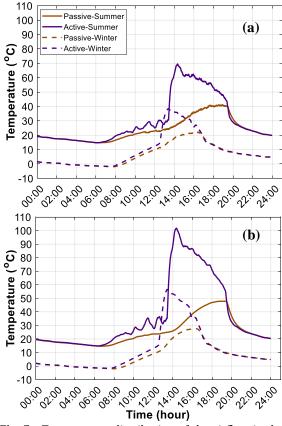

Fig. 5 - Temperature distribution of the airflow in the ventilated cavity (a) middle height, (b) top opening.

3.2 Heat flux through the interior surface

The heat flux through the interior surface of the wall assembly with both passive and active façades in winter and summer is presented in Figure 6. The negative values in the plots indicate that heat leaves the indoor space. According to the results, the heat

flux leaves the room in winter considering wall structure with both cladding types, which was expected due to the higher indoor temperature compared to the outdoor temperature. In summer, however, the heat flux most of the time (except after 22:00) leaves the indoor space of the wall assembly with the passive cladding, which is due to the lower interior surface temperature compared to the indoor temperature. By replacing the external cladding with an active façade, the wall structure may lose or gain heat, depending on the time of the day and the diurnal variation of the interior surface temperature, as it was discussed in section 3.1. The maximum difference in the heat loss of the wall with passive and active façades reaches up to 0.5 W/m² in winter and 1.5 W/m² in summer.
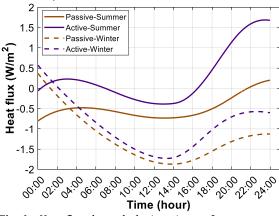

Fig. 6 – Heat flux through the interior surface.

3.3 Airspeed in the cavity

The profiles of the speed of airflow moving in the ventilated air-space are shown in Figure 7. Based on the results, the airspeed in the air gap behind the active façade is most of the time higher compared to the passive cladding. This is due to the higher gradient in the airflow temperature in the cavity behind the active façade caused by the stack effect that is more pronounced during the daytime. The maximum difference between the airspeed in the cavity behind passive and active façades reaches 0.3 m/s in winter and 0.5 m/s in summer. Comparing the results for each cladding type in winter and summer reveals that the airspeed in the ventilated cavity is most of the time higher in the latter, which can be attributed to the higher wind speed (i.e., wind effect) and solar flux (i.e., stack effect) in summer (Figure 3).
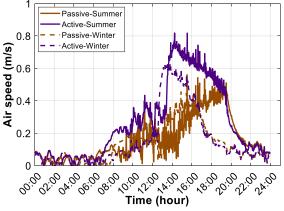

Fig. 7 – Airspeed in the ventilated cavity.

3.4 Heat flow in the cavity

The profiles of the heat flow removed from the air-space are shown in Figure 8. The plots clearly show the higher heat flow passing through the ventilated cavity behind the active façade compared to passive cladding. Interestingly, the cavity behind the BIPV system generates more heat in winter compared to the cavity behind the original cladding of the test building in summer. The maximum heat flow that is removed from the air gap of the wall structure with PV modules reaches 30 kW/m² in winter and 60 kW/m² in summer. The values are much lower in the case of the wooden cladding and do not exceed 10 kW/m². The total amount of heat flow through the cavity behind passive cladding is equal to 16.7 kW/m² on a typical winter day and 33.2 kW/m² on a typical summer day. The corresponding values for the wall assembly with active façade are 77.8 kW/m² and 211.9 kW/m². The results show promising potential for heat recovery behind both cladding types, but more significant in BIPV façade. This aspect is further addressed in the next section.
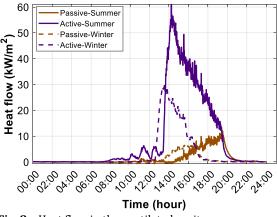

Fig. 8 – Heat flow in the ventilated cavity.

3.5 Heat recovery in the cavity

The heat recovery (i.e., HR in kWh) from the ventilated air-space is calculated using the absolute sum of heat flow through the cavity that could be hourly harvested, considering the area of the cavity with the thickness of 0.07 m and the width of 6.00 m (equation (3)) [26]. It is assumed that the heat flow is uniformly distributed throughout the entire width of the wall.

$$HR = \sum (q_{cav})_{hourly} \times d_{cav} \times w_{cav}/1000 \qquad (3)$$

The results are provided in Figure 9 for representative days in winter and summer. As it is shown, the HR from the ventilated cavity behind the active façade in winter is almost 3 times and in summer 6 times higher than the passive cladding. The HRP in summer is 1.6 times higher than in winter for the cavity behind the passive cladding, while the corresponding value is 2.7 times for the active façade.
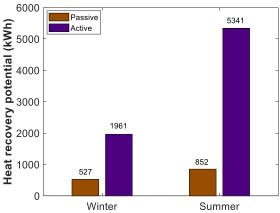
Fig. 9 – Heat recovery in the ventilated cavity.

The results confirm the advantage of replacing passive claddings with active BIPV façades to benefit from the electricity generated by the PV panels and also to achieve the higher potential of the heat flow recovered from the ventilated air cavity. Further analysis is needed to assess the applicability of the heat flow collected from the back of external claddings. The harvested heat from the air gap may have enough thermal energy, which eventually can be used in the subsequent system in the building section. In other words, the preheated air extracted from the air cavity can be used as an additional source to provide ventilation for the room space, reduce the heating load provided by the HVAC system, and increase the water temperature in the hot water supply system. Furthermore, since the airflow in the ventilated cavity has a major impact on the heat recovered, it is necessary to increase the airspeed in the air gap to boost the amount of thermal energy harvested. This could encourage practitioners to take advantage of using a fan system and control the air flow rate in the air gap.

4. Conclusion

The impact of the presence of a ventilated air-space behind a passive wooden cladding and an active BIPV façade on the thermal performance of the wall structure was examined in this study. A transient 2D model was employed, and the simulations were performed for a case study of a building prototype in Fribourg, Switzerland. Two representative days in the winter and summer of 2021 were selected, and the measured weather data was used to numerically investigate the performance of the wall structures assuming fixed standardized indoor temperatures in winter and summer. The results were presented and compared in terms of the temperature distribution through the wall assembly, heat flux through the interior surface of the wall, airspeed in the ventilated air gap, and heat flow passing through the cavity. The heat recovery from the air-space behind both passive and active façades was also evaluated and the possible applications of the harvested heat flow in the building were addressed.

According to the results, the temperature of the active façade becomes higher compared to the passive cladding due to the difference in the thermo-physical properties of materials. The results showed that the thermal mass of the external cladding affects the diurnal variation of the temperature profiles. Moreover, it was revealed that the stack effect has a considerable impact on the air temperature gradient along with the height of the cavity. The results indicated that the heat flux through the interior surface alters between the loss and gains in summer, while the heat always leaves the indoor space in winter. It was shown that the airflow in the cavity driven by the wind-induced and stack effects has a higher speed in the air gap behind the active façade compared to the passive cladding. Consequently, the heat flow within the air-space became higher in the former. Analyzing the heat flow from the ventilated cavity showed that there is a noticeable potential of recovery of the heat energy from the air-spaces, particularly, for the active BIPV façade system in summer.

This study was performed to highlight the possibility of harvesting heat flow from the ventilated air-spaces behind passive and BIPV façade systems. The results confirmed that instead of wasting the potential heat energy of the airflow in the cavity, it could be recovered and further utilized as an additional heat source for the building. The results of this study are provided assuming a wall structure completely covered with the PV modules, while the presence of small air passages between the panels should be considered in future works, which could affect the hydrodynamic behavior of the airflow in the air-space, and consequently, the heat recovery potential. Moreover, the analysis was carried out assuming a uniform distribution of heat flow within the entire width of the wall. Therefore, 3D simulations are recommended to be done in future studies to investigate the impact of non-uniformity of the airflow on the results.

Nomenclature

Symbol	Definition [Unit]
c_p	Specific heat capacity [J/kg K]
d	Thickness of the material [m]
h	Heat transfer coefficient [W/m^2 K]
H	Height [m]
I	Solar radiation [W/m^2]
k	Thermal conductivity [W/m K]
m	Mass flow rate [kg/s]
q	Heat flux [W/m^2]
T	Temperature [℃]
V	Speed [m/s]
w	Width [m]

Subscripts

Symbol	Definition
b	bottom
cav	cavity
ext	exterior
ind	indoor
int	interior
out	outdoor
s	surface
t	top

5. References

1. Aelenei LE. Thermal performance of naturally ventialted cavity walls. Ph.D. dissertation. 2006.
2. Rahiminejad M, Khovalyg D. Impact of the Ventilated Cavity on the Thermal Performance of Traditional Wall Structures. ASHRAE Trans. 2021;127:187-195.
3. Rahiminejad M, Berquand C, Khovalyg D. Transient thermal response of opaque building envelope elements: EPFL campus case study. J Phys Conf Ser. 2021;2042(1):012080.
4. Rahiminejad M, Khovalyg D. In-situ measurements of the U-value of a ventilated wall assembly. J Phys Conf Ser. 2021;2069: 012212.
5. Schindelholz R, Rahiminejad M, Chatterjee A, Khovalyg D. Assessment of thermal and electrical performance of BIPV façades using simplified simulations. J Phys Conf Ser. 2021;2042(1):012081.
6. Rahiminejad M, Khovalyg D. Thermal resistance of ventilated air-spaces behind external claddings; definitions and challenges (ASHRAE 1759-RP). Sci Technol Built Environ. 2021;27(6):788-805.
7. Rahiminejad M, Khovalyg D. Thermal resistance of the ventilated air-spaces behind external claddings; theoretical definition and a parametric study. J Phys Conf Ser. 2021;2069: 012197.
8. Rahiminejad M, Khovalyg D. Measuring the effective thermal resistance of ventilated air-spaces behind common wall assemblies: theoretical uncertainty analysis and recommendations for the hot box method modifications (ASHRAE 1759-RP). Sci Technol Built Environ. 2022;in press.
9. Straube J, Finch G. Report 0906: Ventilated wall claddings: review, field performance, and hygrothermal modeling. Test. 2009:25. www.buildingscience.com.
10. Bikas D, Tsikaloudaki K, Kontoleon KJ, Giarma C, Tsoka S, Tsirigoti D. Ventilated Facades: Requirements and Specifications Across Europe. Procedia Environ Sci. 2017;38:148-154.
11. Straube JF, Straaten R van. Field Studies of Ventilation Drying. 2004;47(11-12):387-406.
12. Zogou O, Stapountzis H. Flow and heat transfer inside a PV/T collector for building application. Appl Energy. 2012;91(1):103-115.
13. Rahiminejad M, Khovalyg D. Dynamic Thermal Performance of the BIPV Facades. ASHRAE Trans. 2021;127:170-178.
14. Richman RC, Pressnail KD. A more sustainable curtain wall system: Analytical modeling of the solar dynamic buffer zone (SDBZ) curtain wall. Build Environ. 2009;44(1):1-10.
15. Diallo TMO, Zhao X, Dugue A, et al. Numerical investigation of the energy performance of an Opaque Ventilated Façade system employing a smart modular heat recovery unit and a latent heat thermal energy system. Appl Energy. 2017;205:130-152.
16. Rounis ED, Bigaila E, Luk P, Athienitis A, Stathopoulos T. Multiple-inlet BIPV/T modeling: Wind effects and fan induced suction. Energy Procedia. 2015;78:1950-1955.
17. Hailu G, Dash P, Fung AS. Performance evaluation of an air source heat pump coupled with a building-integrated photovoltaic/thermal (BIPV/T) System under cold climatic conditions. Energy Procedia. 2015;78:1913-1918.
18. Dehra H. An investigation on energy performance assessment of a photovoltaic solar wall under buoyancy-induced and fan-assisted ventilation system. Appl Energy. 2017;191:55-74.
19. Ahmed-Dahmane M, Malek A, Zitoun T. Design and analysis of a BIPV/T system with two applications controlled by an air handling unit. Energy Convers Manag. 2018;175:49-66.
20. Rahiminejad M, Paris A, Ge H, Khovalyg D. Performance of lightweight and heavyweight building walls with naturally ventilated passive and active facades. Energy Build. 2022;256:111751.
21. Rahiminejad M, Khovalyg D. Review on ventilation rates in the ventilated air-spaces behind common wall assemblies with external cladding. Build Environ. 2021;190:107538.
22. Finch G. The Performance of Rainscreen Walls in Coastal British Columbia. Univ Waterloo. 2007.
23. SIA (2015). Standardized data for building energy modeling (SIA 2024:2015). Zurich, Switzerland.
24. Agathokleous R. Thermal Analysis of naturally ventilated BIPV systems. Ph.D. dissertation. 2017.
25. Gan G. Numerical determination of adequate air gaps for building-integrated photovoltaics. Sol Energy. 2009;83:1253-1273.
26. Girma GM, Tariku F. Experimental investigation of cavity air gap depth for enhanced thermal performance of ventilated rain-screen walls. Build Environ. 2021;194:107710.

Data Statement